Atmospheric Chlorine Reaction with N-Methyl-2-Pyrrolidinone (NMP)

S. Samai
université Abess Laghrour
A. Ferhati (azeddine.ferhati@univ-batna.dz)
université de Batna

Research Article

Keywords: Atmospheric, DFT, NMP, DMA

Posted Date: April 20th, 2021

DOI: https://doi.org/10.21203/rs.3.rs-433706/v1

Atmospheric Chlorine Reaction with N-methyl-2-pyrrolidinone (NMP)

S. Samai*[1-2], A. Ferhati*[1]

[1]LCCE Laboratoire de chimie et chimie de l'environnement, faculté des sciences, département de chimie, université de Batna, 05000 Batna Algérie

[2]Faculté des sciences et Technologie, département de Science de la Matière, université Abess Laghrour, 40000 Khanchela-Algérie

***Corresponding authors.**

E-mail address: *azeddine.ferhati@univ-batna.dz, salima_samai@hotmail.fr,*

ABSTRACT:

Density functional theory (DFT) and Complete Basis Scale methods (CBS-QB3, G3B3) are used to investigate the reactivity, the mechanism, structure-reactivity relationship and the kinetics of N-methyl-2-pyrrolidinone (NMP) with Cl atom. To obtain rate constants of the reaction, the RRKM theory is employed at atmospheric pressure and temperature range 273–380 K. This study provides the rate coefficients and detailed H-abstraction mechanism for the reaction of Cl with NMP at high level of theoretical methods. The obtained rate constant ~ 0.92 x 10^{-10} to 8.98 × 10^{-10}cm ^{3} molecule^{-1}s^{-1} at 298 K agreed with those obtained previously for N,N-dimethyl formamide (DMF) and N,N-dimethyl acetamide (DMA). The study shows that the reaction mechanism of Cl with NMP goes favorably through an H-abstraction from N-methyl groups and adjacent CH_2. The rates constants obtained for the three amides confirm our prediction regarding the structure-reactivity relationship where 1000/T.

1. Introduction

Chlorine reactions with volatile organic compounds (VOCs) are important for the atmospheric observations regarding the pollution of the troposphere and has provided models for studies of dynamics and kinetics of reactions in gas phases. In the troposphere, VOCs constitute a major class of chemicals emitted directly into the earth's troposphere. The H-abstraction from these compounds provides an important source of O_3 and other photochemical pollutants in coastal and industrialized areas [1].

Amides form a wide variety of volatile organic nitrogen compounds (NVOCs). They are considered as primary pollutants or secondary pollutants [2]. Amides reactions with atmospheric radicals shows the involvement of these contaminants relative to the tropospheric lifetime in relation to each atmospheric photo-oxidant [1–5].

Koch et al. [6], Aschmann et al. [7] Solignac et al. [8], and El Dib et al [9] carried out the reaction of amides with atmospheric oxidants. Koch et al. [6] used flash/fluorescence resonance photolysis to study the oxidation kinetics of amides by OH radicals at various temperatures. Aschmann et al. [7] used the relative rate technique to study the OH and NO_3 homogeneous oxidation kinetics of N-methyl-2-pyrrolidinone. Solignac et al. [8] have determined the kinetics reactions of the amide with OH radical and Cl at room temperature. G. El Dib et al. [9] studied the radical reaction of NO_3 with certain amides at different temperatures and determined the rate coefficient by laser photolysis coupled with UV-visible spectroscopy and time resolved absorption. The kinetic results without a mechanism investigation (isotope labelling) seems indicate that the reactions of amides with atmospheric oxidants is sensitive to the amide structure.

NMP, with low volatility and high chemical and thermal stability, is considered to replace some organic solvents[6]. Few information exist concerning the mechanisms of amides degradation by atmospheric oxidants. Mechanistic and theoretical studies are useful to give an understanding of the mechanism involved in reaction process with atmospheric radicals. This study reports a theoretical investigation of the kinetics and structure-reactivity mechanism of Cl atom with NMP a cyclic amide.

The results reported provide additional information on the kinetics of the reaction with atmospheric oxidants to understand the tropospheric implication of NMP and its importance as a primary or secondary pollutant.

2. Theoretical Methods

2.1. Quantum Chemistry Calculations

The calculations obtained using the Gaussian 09 package[10] available at the URCA-France and the data analysis were done on the CPO platform at the U-BATNA-1 in Algeria. Geometries and electronic structures for all minimas and transition states (TS) were calculated with density functional theory DFT B3LYP/6-311++G(2d,pd) level of theory[11].

Each stationary point was determined by calculating the frequencies harmonic vibration and the minimum is characterized by real frequency, the reaction TS's are localized with the "quasi-Newton guided by

synchronous transit" procedure for the search for the saddle point (QST3). The Hessian matrix of TS has a one negative frequency. The localization of the TS as recommanded in a previous criticism were confirmed with intrinsic reaction coordinates calculations (IRC)[12].

As B3LYP method overestimates H-abstraction barriers and provides unreliable thermochemical values. The neutrals, radicals, and transition-states geometries were optimized using B3LYP method, CBS-QB3 model of Petersson et al [13-23] was used to calculate the energies of the different species involved. In fact, current studies show that the CBS-QB3 method frequently gives good agreement with experimental reaction energies and barriers for molecules having same size to those involved in this work [24-26]. Heats of formation for all gaseous species involved in the reaction were calculated based on the procedure defined in the literature [24-25].

G3B3 (or G3//B3LYP), a variant of G3 method, is useful for larger open-shell systems with a very low spin contamination (~1 kcal/ mol for the neutral set of molecule)[26]. Enthalpies of formation at 0 K and 298 K were calculated as defined in our previous work. [26-29].

2.2. Rate Calculations.

The rate constants were carried out using RRKM theory[30-32] counting the required sums, density of states, frequencies, zero-point energies and moments of inertia. Kinetics calculations were done with reactants, TSs, and products optimized at B3LYP/6-311++G(2d,pd) level of theory. Enthalpies calculated from both CBS-QB3//B3LYP/6-311++G(2d,pd) and G3B3// B3LYP/6-311++G(2d,pd) for all gaseous species injected in the Master equation (ME in Chemrate) permit to obtain the rates constants including the temperature dependence for each reaction involved in the global mechanism[33-41]. Our simulations take the most stable conformer. These simplifications will have little effect on numerical precision but should affect the validity of the rates values obtained.

3. Structural calculations

Five stationary points on the profile energy surface (PES) have been localized,with a competition of four H-abstraction pathways, for each path: the reactants,the reactant complex, the transition state, the product complex and the products respectively NMP, HCL, CR1-CR4, TS1-TS4, CP1-CP4 and P1-P4.

For N-methyl-2-pyrrolidinone (NMP), H-abstraction may take place (Figure1) at several sites**.** The reaction is estimated to process with H- abstraction from the three −CH2 − groups of the pentacycle, or −CH3 adjacent to the Nitrogen. The TS's geometry consist of a near-linear alignment of the Cl atom, the H atom to be abstracted, and the atom to which the H atom is attached in the neutral structure. Four channels have been modeled for NMP +Cl.

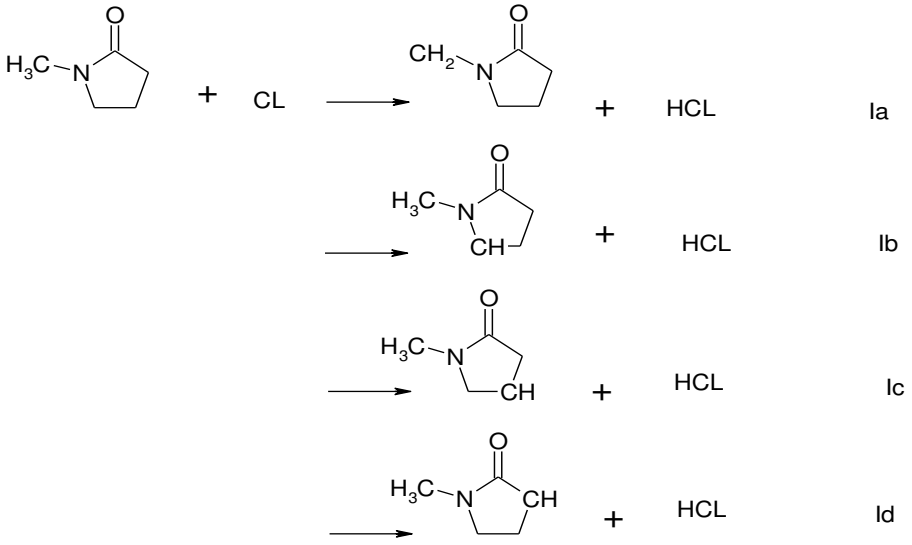

The reaction H-abstraction pathways progress via three-steps, namely: (i) the formation of the complex CR1-CR4 from the isolated reactants NMP+Cl, (ii) the formation of the complex CP1-CP4 from the reactant complex through the TS1-TS4 and (iii) the formation of the consistent radical and HCl from the product complex Fig 1−4. Table 1-6 regroup the energies of reactants, complex reactants , Ts's, complex products and products species involved in the mechanism.

The experimental and theoretical enthalpies are in good agreement except for R1–R4 species **Fig 1** for which the experimental enthalpies are not available in the literature as mentionned previously in [26-29].

3.1 H-Abstraction from –N-CH₃ group.

The H abstraction in this path includes only one H from the CH_3 of the –N-CH_3 group of the amide. The TS1 characterized by a single imaginary frequency of -534.94 cm^{-1} is confirmed by the IRC calculation (see supporting information). The reactive complex CR1 is energetically stable, The C -H bond distance in this reactive complex (RC1) is ~1.20 Å and the intermediate hydrogen bond C-H…Cl is ~1.82 Å, while for TS1, the distances of identical bond are respectively ~1.41 and ~1.42 Å. The CP1 involve an inter molecular H bond between the carbon atom and HCl with a distance of ~1.62 Å. This path involves an energy barrier of ~6, 44 (**6,17**) kcal / mol.(in parentheses and bold the energy barrier at G3B3 // B3LYP / 6-311 G- (2d, pd) level) The reaction path is exothermic and exergonic see Table 4.

3.2 H-Abstraction from −CH_2 adjacent to the N-CH_3 group

In this path the H- abstraction process includes the hydrogen of the −CH_2- group adjacent to the N-CH_3. The CP2 structure shows an intermolecular H-bond between the carbon of the group -CH_2- adjacent to the N-CH_3 and HCl with a bond distance of ~1.66 . The C-H bond in the CR2 is ~1.20 Å, the like bond H…Cl distance is ~1.81 Å while for the TS2 the distances bonds involved in the coordinate reaction are, respectively, ~1.40 and ~1.42 Å. The CP2 via dissociation of the intermolecular H-bond gives rise to the product P2 and HCl. This path involves an energy barrier of ~12,70 (**8,33**) kcal / mol. The reaction process is exothermic and exergonic (seeTable 4) as in the previous path .

3.3 H-Abstraction from Group −CH_2 central and −CH_2 adjacent to the C=O group

The H- abstraction process in this path includes the hydrogen of the CH_2- group central in the NMP structure. The products complex involve an intermolecular hydrogen bond between the carbon atom of the CH_2- and HCl with a bond distance of ~1.66 and 1.68 respectively for CP3 and CP4 . The bond distance C-H in the reactive complex is ~1.27 Å while the like bond H…Cl distance is ~1.80 to 1.81 Å for both. The distances bonds involved in the two TSs are, respectively, ~1.40 and ~1.45 Å. These reactions involves energies barriers of ~20.97 (**32.72**) kcal / mole for TS3 and ~19.99 (**31.11**) kcal / mole for TS4. For theses path's, although the reactions process are lightly exothermic and exergonicsee (see Table 4) , the calculations shows a very high barrier compared to the other paths and were not taken in

consideration in the Kinetic calculations without considering the tunneling effect that may occur in these cases.

4. KINETICS

The mechanism of H-abstraction reaction of NMP with Cl is studied as a competition between two H-abstractions as follows.

$$NMP + Cl \underset{k'_{-Ia}}{\overrightarrow{k_{Ia}}} (CR)_I \overrightarrow{k_{Ib}} (CP)_I \underset{k'_{-Ic}}{\overrightarrow{k_{Ic}}} P1 + HCl$$

$$\underset{k'_{-IIa}}{\overrightarrow{k_{IIa}}} (CR)_{II} \overrightarrow{k_{IIb}} (CP)_{II} \underset{k'_{-IIc}}{\overrightarrow{k_{IIc}}} P2 + HCl$$

as seen previously in the Cl reaction with DMF and DMA, and according to the PES's, the rate constant (k) of the four channels can be analyzed in terms of conventional transition-state theory (CTST) or RRKM/ME calculations. k_{Ia}, k_{IIa}, represent the forward rates, k_{-Ia}, k_{-IIa} k_{Ib}, k_{IIb} the reverse ones for the first step and the second step respectively for channel Ia, while k_{Ic}, k_{IIc}, represent the forward rates and k_{-Ic}, k_{-IIc} the reverse ones for channels Ib.

Rate constants (k_I, k_{II}) of channels Ia−Ib can be obtained according to this hypothesis, as:

$$k_I = k_{eqIa} \times k_{Ib} \times k_{eqIc} \qquad (a)$$

$$k_{II} = k_{eqIIa} \times k_{IIb} \times k_{eqIIc} \qquad (b)$$

Where k_{eqIa}, k_{eqIIa}, k_{eqIc}, k_{eqIIc}, represent the equilibrium constants connecting the isolated reactants and the complexes for channel I and channel II respectively.

The rates constants involved in the H-abstraction mechanism were carried out with ChemRate program [14]. Simulations were determined at 1atm and 273- 380 K. Collision energy transfer was designated by an exponential-down model, with ΔE_{down}=300 cm^{-1}, Ar (argon) considered as bath gas with lennard-jones parameters of σ=4.4 and ξ=216 K [38-39]. All rate constants obtained in this study are in s^{-1} or cm^3 $molecule^{-1}$ s^{-1} units.

The $k_{overall}$ (c), the branching ratios (d) obtained from the kinetic simulation model are calculated as follow

$$k_{\text{overall}} \leq k_I + k_{\text{II}} \qquad \text{(c)}$$

$$\beta_I = \frac{k_I}{k_I + k_{\text{II}}}, \beta_{\text{II}} = 1 - \beta_I \qquad \text{(d)}$$

The calculations of the transmission coefficients (□□□, using the Wigner, Skodje, and Truhler formalisms[42-43] were obtained in the range 278−400 K. Small tunneling effect was observed (0.994 to 1.004) saying no effect on the rate constant values calculated in this study as seen in our previous work for DMF and DMA[28].

5. RESULTS AND DISCUSSION

The H-abstraction from N-methyl -2-pyrrolidinone (NMP) reaction as described above, has been modeled according to a complex mechanism in the entrance channel: two complexes CR1 and CR2 have been considered with the lowest two transition states TS1 and TS2 respectively followed by two complexes CP1 and CP2 for each reaction profile.

The H-abstraction from the –N-CH_3 group site leads to the species PC1. This path was found to be slightly dominant with a branching ratio $\beta_I = 0{,}55$, as for DMA, toward electrophilic attack due to the positive inductive effect of these groups can be stated for this reaction. Significant negative temperature effect was

noted for k_I and k_{II}. $k_{overall}$ vary from 8.87(E-10) to 1,05(E-09) cm^3 $molecule^{-1}s^{-1}$ in the temperature range 273-380 K (see Table 5-6). The linear fit of all the data carried out using the calculation at different temperatures; leads to the Arrhenius expression at CBS-QB3 and G3B3 level of theory equation e and f (see Fig 5):

$$k_{overall}(T) = 8.89 \times 10^{-10} * exp(-163.8/T)\ cm^3\ molecule^{-1}s^{-1} \quad (e)$$

$$k_{overall}(T) = 3.70 \times 10^{-11} * exp(63.8/T)\ cm^3\ molecule^{-1}s^{-1} \quad (f)$$

Previous studies have focused on the reactivity of DMF (N,N-dimethyl formamide $(CH_3)_2NCOH$) and DMA (N,N-dimethyl acetamide $(CH_3)_2NC(O)CH_3$)) with OH radical and Cl. Only one experimental study on the reactivity of NMP was carried out by Aschmann et al.[7], the relative rate technique was used for the homogeneous oxidation kinetics of NMP with OH and NO_3.

Theoretical and mechanistic investigation of the reactions of DMF and DMA with Cl, OH and NO3 published previously[28] gives rate constants of 4.45×10^{-10} and 9.92×10^{-10} $cm^3 molecule^{-1}s^{-1}$ at 298 K respectively obtained with the DFT//CBS-QB3//B3LYP/6-311++G(2d,pd) level of theory. The results are in the same order with the ones observed for NMP and shows that there is a relation between the rate constant and the structure of the amides (reactivity-structure relationship): $k_{NMP} > k_{DMF} > k_{DMA}$

The rate constant of the reaction of Cl with NMP decrease as the temperature increases in the range 273-380 K and are in good agreement with the results of the reaction Cl with DMF and DMA[28]. In the literature the reaction of DMA and DMF with CL [8], state that for DMA and DMF, abstraction occur with a branching ratio of 55 %, in N-CH3 groups [28]. This mechanistic tendency is also observed in the theoretical calculations, where the H-abstracted from the –N-CH3 group appeared to be slightly dominant channel with small barrier energy and negative temperature dependence. For the reaction of NMP with Cl over the temperature range explored, an important effect of the temperature is observed.

6. Conclusion

This study represents a theoretical determination of the rate coefficients and detailed H-abstraction mechanism for the reaction of the Chlorine atom with one cyclic amide (NMP), within the temperature range 273–380 K. This work has been achieved using high level of theory DFT, CBS-QB3 and G3B3 methods considered to be the most efficient and accurate computational methods for the study of this kind of reactions. The reaction of NMP with Cl is exothermic and exergonic taking place in five steps as mentioned in our previous work for DMF and DMA. Kinetic and mechanistic results show that the mechanism of the Cl reaction with NMP goes with small barriers through H-atom transfer from –N-CH_3 group and -CH_2 adjacent to the N-CH3 site within a branching ration slightly in favor of the N-CH3 site. The suggested mechanism is maintained by the results for reactions of DMF and DMA with chlorine [28]. The rate constants determined in this study present a troposphere lifetime of 3 to 10 days which could be seen as affect the chemistry of the troposphere on local and regional scales.

Supporting Informations

Acknowledgment

Thanks to MESRS and DGRSDT Algeria

Grateful thanks to Pr. Chakir Abdelkhaleq from GSMA Reims-France

References

[1] Manahan, S.E. Environmental Chemistry. Lewis, London. 1994

[2] Carter, W.P.L. J. Air Waste Manage. Assoc. 1994, 44, 881.

[3] Finlayson-Pitts, B.J., Pitts Jr., J.N.,. Chemistry of the Upper and Lower Atmosphere. Academic Press, California.1999

[4] Matsunaga, S. N.; Wiedinmyer, C.; Guenther, A. B.; Orlando, J. J.; Karl, T.; Toohey, D. W.; Greenberg, J. P.; Kajii, Y. Isoprene oxidation products are a significant atmospheric aerosol component. Atmos. Chem. Phys. Discuss. 2005, 5, 11143.

[5] Tuazon, E.C., Atkinson, R., Aschmann, S.M. The kinetics and products of the gas-phase reactions of O 3 with a series of aliphatic amines and related compounds, Res. Chem. Intermed. 1994, 20, 303.

[6] Koch, R., Palm, W.U., Zetzsch, C. First-rate constants for reactions of OH radicals with amides Int. J. Chem. Kinet. 1997, 29, 81–87.

[7] Aschmann, M.S., Atkinson, R. Atmospheric chemistry of 1-methyl-2-pyrrolidinone Atmos. Environ. 1999, 33, 591–599.

[8] Solignac, G., Mellouki, A., Le Bras, G., Barnes, I., Benter, Th. Kinetics of the OH and Cl reactions with N-methylformamide, N,N-dimethylformamide and N,N-dimethylacetamide. J. Photochem. Photobiol. A 2005, 176, 136–142.

[9] El Dib, G., Chakir, A. Temperature-dependence study of the gas-phase reactions of atmospheric NO 3 radicals with a series of amides Atmos. Environ. 2007, 41, 5887–5896.

[10] Frisch, M. J.; Trucks, G. W.; Schlegel, H. B.; Scuseria, G. E.; Robb, M. A.; Cheeseman, J. R.; Scalmani, G.; Barone, V.; Mennucci, B.; Petersson, G. A.; Nakatsuji, H.; Caricato, M.; Li, X.; Hratchian, H.P.; et al. Gaussian 09, revision B.01; Gaussian, Inc.: Wallingford, CT,2010.

[11] Lee, C.; Yang, W.; Parr, R. G. Development of the Colle-Salvetti correlation-energy formula into a functional of the electron density.Phys. Rev. B: Condens. Matter Mater. Phys. 1988, 37, 785.

[12] (a) Gonzalez, C.; Schlegel, H. B. An improved algorithm for reaction path following. J. Chem. Phys. 1989, 90, 2154. (b) Gonzalez, C.; Schlegel, H. B. Reaction path following in mass-weighted internal coordinates. J. Phys. Chem. 1990, 94, 5523.

[13] Montgomery, J. A.; Frisch, M. J.; Ochterski, J. W.; Petersson, G. A. A complete basis set model chemistry. VI. Use of density functional geometries and frequencies,. J. Chem. Phys. 1999, 110, 2822.

[14] Coote, M. L.; Wood, G. P. F.; Radom, L. Methyl Radical Addition to CS Double Bonds: Kinetic versus Thermodynamic Preferences. J. Phys. Chem. A 2002, 106, 12124.

[15] Dybala-Defratyka, A., Paneth, P., Pu, J., Truhlar, D.G. Benchmark Results for Hydrogen Atom Transfer between Carbon Centers and Validation of Electronic Structure Methods for Bond Energies and Barrier Heights J. Phys. Chem. A 2004, 108, 2475

[16] Olzmann, M.; Kraka, E.; Cremer, D.; Gutbrod, R.; Andersson, S. Energetics, Kinetics, and Product Distributions of the Reactions of Ozone with Ethene and 2,3-Dimethyl-2-butene. J. Phys. Chem. A 1997, 101, 9421.

[17] Fenske, J. D.; Kuwata, K. T.; Houk, K. N.; Paulson, S. E. Formation of the OH Radical in the Reaction of Ozone with Several Cyclo-alkenes. J. Phys. Chem. A 2000, 104, 7246.

[18] Kroll, J. H.; Sahay, S. R.; Anderson, J. G.; Demerjian, K. L.; Donahue, N. M. Mechanism of HOx Formation in the Gas-Phase Ozone-Alkene Reaction. J. Phys. Chem. A 2001, 105, 4446.

[19] Zhang, D.; Lei, W.; Zhang, R. Mechanism of OH formation from ozonolysis of isoprene: kinetics and product yields. Chem. Phys. Lett. 2002, 358, 171. 514

[20] Wood, G.P.F., Henry, D.J., Radom, L. Performance of the RB3-LYP, RMP2, and UCCSD(T) Procedures in Calculating Radical Stabilization Energies for •NHX Radicals J. Phys. Chem. A 2003, 107, 7985.
[21] Fenske, J. D.; Hasson, A. S.; Paulson, S. E.; Kuwata, K. T.; Ho, A.; Houk, K. N. The pressure dependence of the OH radical yield from ozone alkene reactions. J. Phys. Chem. A 2000, 104, 7821.
[22] Cremer, D.; Kraka, E.; Szalay, P. G. Decomposition modes of dioxirane, methyldioxirane and dimethyldioxirane A CCSD (T), MR-AQCC and DFT investigation. Chem. Phys. Lett. 1998, 292, 97.
[23] Petersson, G. A. ; Malick, D. K.; Montgomery, J. A. Transition states for chemical reactions I. Geometry and classical barrier height. J. Chem. Phys. 1998, 108, 5704.
[24] Stipa, P, The reactivity of aminoxyls towards peroxyl radicals: an ab initio thermochemical study J. Chem. Soc., Perkin Trans. 2001, 2, 1739.
[25] Tiu, Gerald C., Tao, Fu-Ming. Theoretical mechanisms and kinetics of the hydrogen abstraction reaction of acetone by chlorine radical Chem. Phys. Lett. 2006, 428, 42–48.
[26] Robinson, P.J., Holbrook, K.. Unimolecular Reactions. Wiley-Interscience, London . 1972.
[27] Curtiss, L.A., Raghavachari, K., Redfern, P.C., Pople, J.A. Assessment of Gaussian-2 and density functional theories for the computation of enthalpies of formation J. Chem. Phys. 1997, 106, 1063.
[28] Samai, S.; Rouichi, S.; Ferhati, A.; Chakir, A. N,N- dimethylformamide (DMF), and N,N-dimethylacetamide (DMA) reactions with NO3, OH and Cl: A theoretical study of the kinetics and mechanisms,. Arabian J. Chem. 2016, DOI: 10.1016/ j.arabjc.2016.10.012.
[29] S. Rouichi, S. Samai, A. Ferhati, A. Chakir. Atmospheric Reaction of Cl with 4−Hydroxy-2-pentanone (4H2P): A Theoretical Study. *J. Phys. Chem. A* 2018, 122, 8, 2135-2143
[30] Mokrushin, V.; Bedanov, V.; Tsang, W.; Zachariah, M. R.; Knyazev, V. D. CHEMRATE, version 1.19; National Institute of Standards and Technology: Gaithersburg, MD, 2002.
[31] Tsang, W.; Bedanov, V.; Zachariah, M. R. Master Equation Analysis of Thermal Activation Reactions: Energy-Transfer Constraints on Falloff Behavior in the Decomposition of Reactive Intermediates with Low Thresholds. J. Phys. Chem. 1996, 100, 4011.
[32] Knyazev, V. D.; Tsang, W. Chemically and Thermally Activated Decomposition of Secondary Butyl Radical. J. Phys. Chem. A 2000, 569 104, 10747.
[33] Knyazev, V. D.; Tsang, W. Isothermal Kinetics at Constant Pressur. J. Phys. Chem. A 1999, 103, 3944.
[34] Tokmakov, I. V.; Lin, M. C. Reaction of Phenyl Radicals with Acetylene: Quantum Chemical Investigation of the Mechanism and575 Master Equation Analysis of the Kinetics. J. Am. Chem. Soc. 2003, 125, 11397.
[35] Tokmakov, I. V.; Lin, M. C. Combined Quantum Chemical/ RRKM-ME Computational Study of the Phenyl + Ethylene, Vinyl + Benzene, and H + Styrene Reactions. J. Phys. Chem. A 2004, 108, 9697.

[36] Da silva, G.; Hamdan, M. R.; Bozzelli, J. W. Oxidation of the benzyl radical: mechanism, thermochemistry, and kinetics for the reactions of benzyl hydroperoxide. J. Chem. Theory Comput. 2009, 5, 3185−3194.
[37] Miyoshi, A. Computational studies on the reactions of 3-butenyl and 3-butenylperoxy radicals. Int. J. Chem. Kinet. 2010, 42, 273−288.
[38] Galano, A. Isopropyl cyclopropane + OH Gas Phase Reaction: A Quantum Chemistry + CVT/SCT Approach. J. Phys. Chem. A 2006, 110, 9153−9160.
[39] Wigner, E. P. Uber die paramagnetische Umwandlung von Para- Orthowasserstof. Phys. Chem. B 1932, 19, 203−216.
[40] Skodje, R. T.; Truhlar, D. G. Parabolic tunneling calculations. J. Phys. Chem. 1981, 85, 624.
[41] Aslan, L.; Priya, A. M.; Sleiman, C.; Zeineddine, M. N.; Coddeville, P.; Fittschen, C.; Ballesteros, B.; Canosa, A.; Senthilkumar, L.; El Dib, G.; Tomas, A. Experimental and theoretical investigations the kinetics and mechanism of the Cl + 4-hydroxy-4-methyl-2- pentanone reaction. Atmos. Environ. 2017, 166, 315−326.
[42] Uber die paramagnetische Umwandlung von Para-Orthowasserstof E.P. Wigner *Phys. Chem. B, 19* (**1932**), 203-216.
[43] Parabolic tunneling calculations R.T., Skodje, D.G., Truhlar, *J. Phys. Chem. 85,* (**1981**), 624.

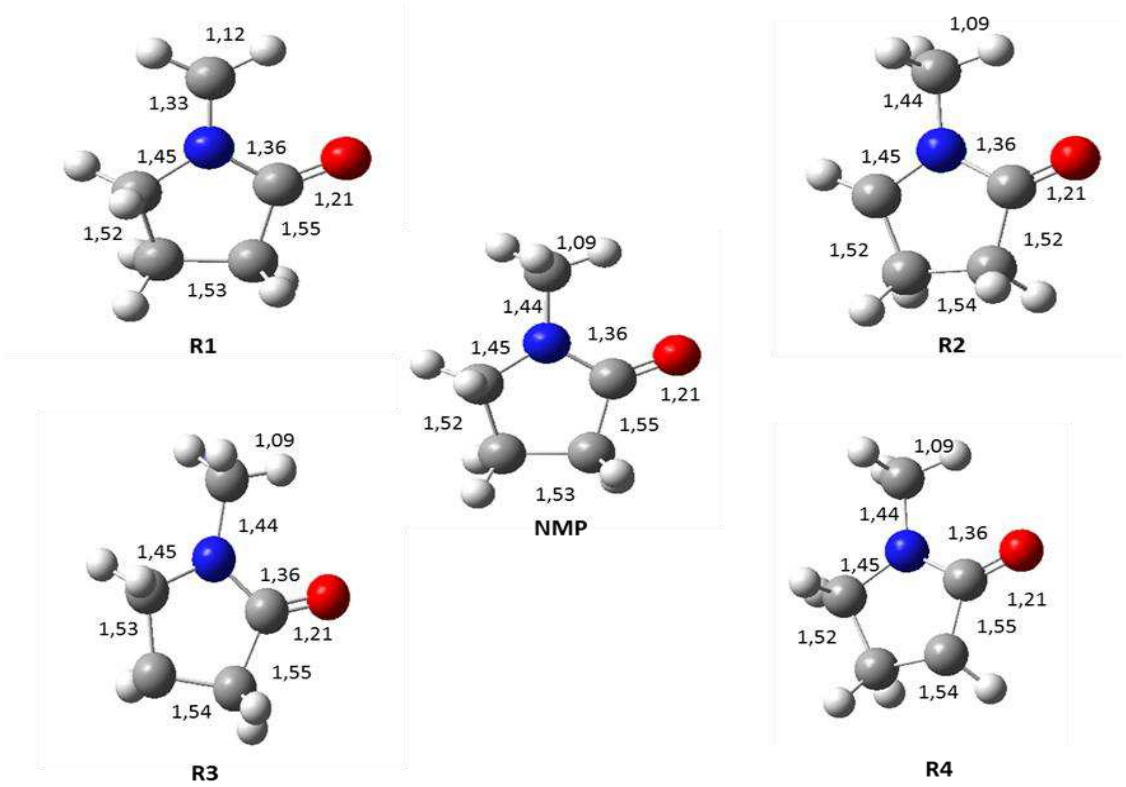

Figure 1. Structures of key species (1-methyl -2-pyrrolidinone –NMP-) and P1−P4 (radicals obtained via channels Ia−Id)) considered for kinetics simulations determined by B3LYP/6-311++G(2d,pd); bond lengths in angstroms.

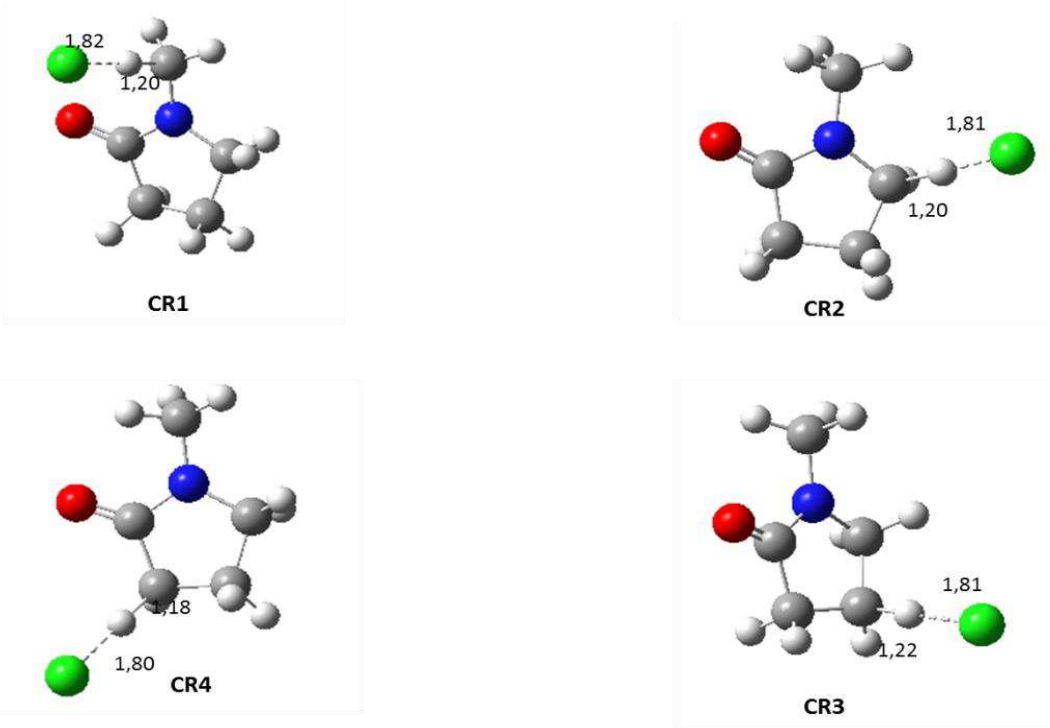

Figure 2. Structures of key species CR1−CR4 (radicals obtained via channels Ia−Id) considered for kinetics simulations determined by B3LYP/6-311++G(2d,pd); bond lengths in angstroms.

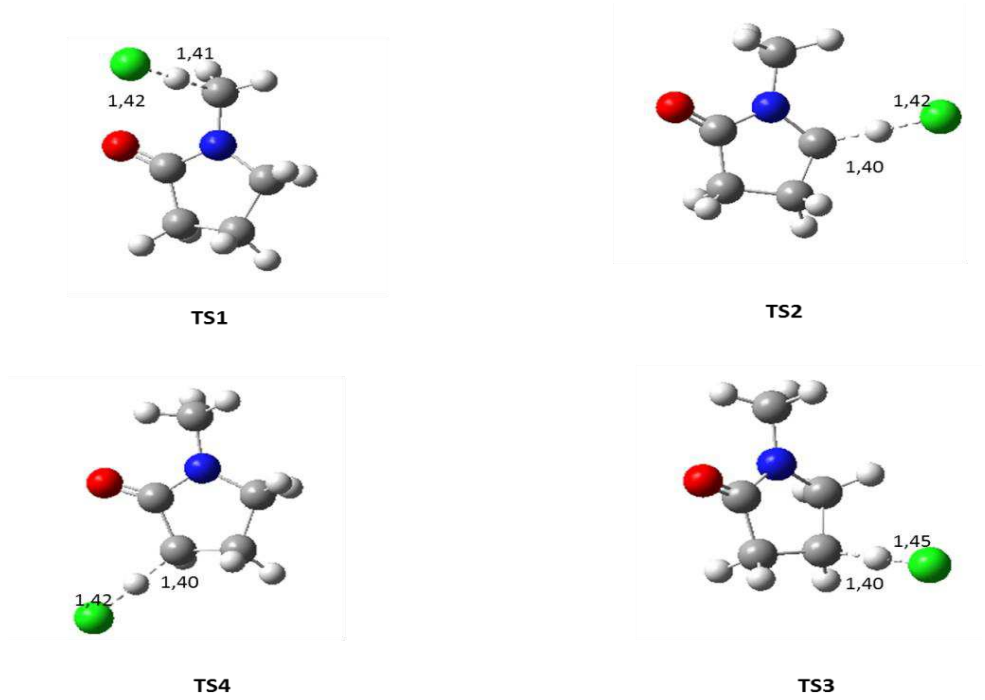

Figure 3. Structures of key species TS1−TS4 (Transitions stat obtained via channels Ia−Id) considered for kinetics simulations determined by B3LYP/6-311++G(2d,pd); bond lengths in angstroms

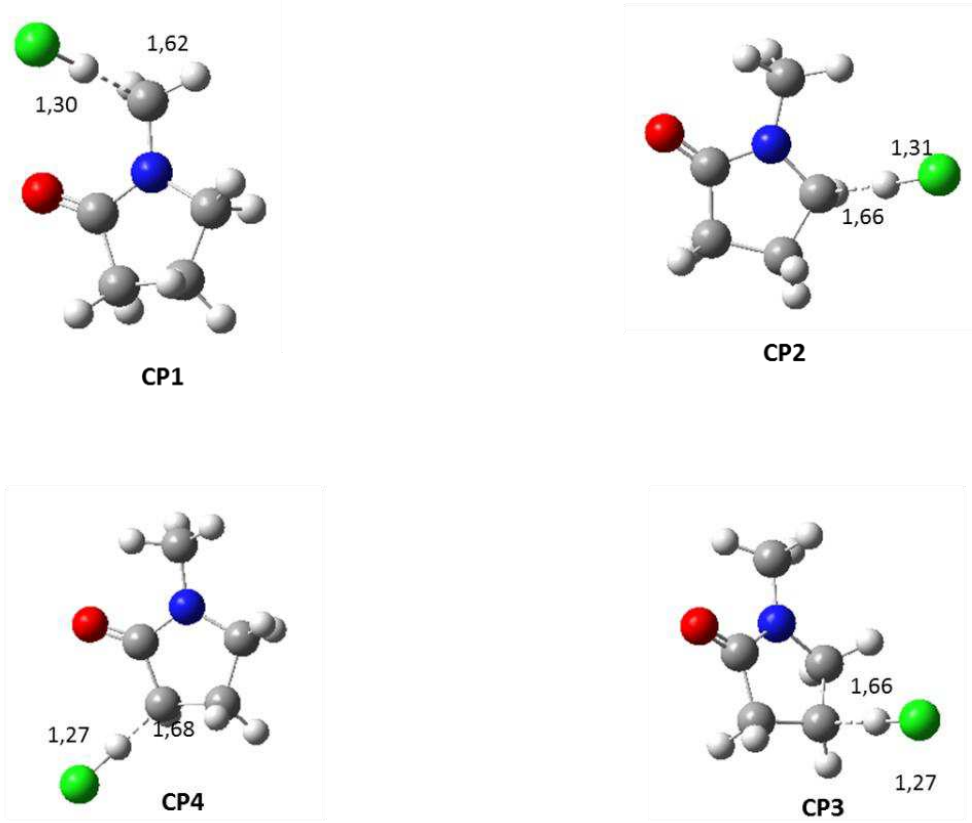

Figure 4. Structures of key species CP1−CP4 obtained via channels Ia−Id considered for kinetics simulations determined by B3LYP/6-311++G(2d,pd); bond lengths in angstroms

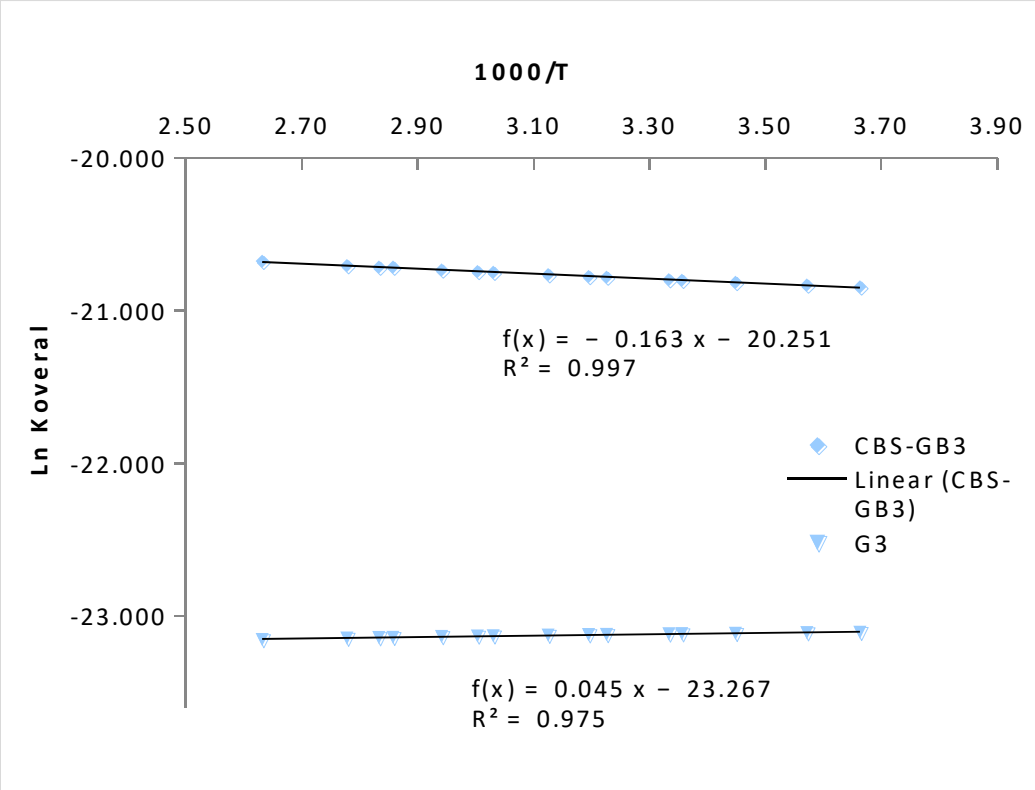

Figure 5. Arrhenius plot $\ln(k_{overall})$ versus 1000/T for NMP + Cl reaction at CBS-QB3 and G3B3

Table 1: Energies (Hartree) of reactants and products species involved in the mechanism : In hartree(u.a) as obtained from the DFT calculation. CBS-H enthalpy at 2 98.15 K. CBS-G Gibbs free energy at 298.15 K. CBS-E energy.CBS (0 K) energy at 0 K. [a] Atomization energy in kcal mol-1 at 0 K. .[b] Heat of formation at 0 K in kcal mol^{-1} . [c]Heat of formation at 298.15 K in kcal mol^{-1}[d] Experimental Heat of formation at 298.15 K in kcal mol^{-1}. (1) CRC Handbook of Chemistry and Physics New York October 2003.

	E-DFT	CBS-H	CBS-G	CBS-E	CBS-0K	D_0[a]	$\Delta H°f_{(0K)}$[b]	$\Delta H°f_{(298K)}$[c]	$\Delta_f H^d_{298K}$
NMP	-326,049078	-325,365587	-325,408694	-325,366531	-325,374519	1591,38	-105,29	-112,10	-107,51
R1	-325,3920739	-324,719681	-324,75868	-324,720625	-324,727539	1499,03	-64,57	-71,05	/
R2	-325,3939165	-324,720451	324,764413	324,721395	-324,72952	1500,27	-65,81	-71,53	/
R3	-325,3672691	-324,693336	-324,732936	-324,69428	-324,701326	1482,58	-48,12	-54,52	/
R4	-325,3727367	-324,699291	-324,740413	-324,700235	-324,7078	1486,64	-52,18	-58,26	/
CL	-459,477436	-459,681285	-459,699322	-459,67646	-459,683645	0,00	28,59	28,61	28,97
HCL	-460,100058	-460,344912	-460,366099	-460,345856	-460,348216	103,38	-23,16	-23,20	-23,04

Table 2: Energies (Hartree) of species involved in the Mechanism Obtained at CBS-QB3//B3LYP/6-311G++(2d,pd) Level . CBS-H enthalpy at 2 98.15 K. CBS-G Gibbs free energy at 298.15 K. CBS-E energy .CBS (0 K) energy at 0 K. [a] Atomization energy in kcal mol-1 at 0 K. .[b] Heat of formation at 0 K in kcal mol^{-1} . [c] Heat of formation at 298.15 K in kcal mol^{-1}.

	E-DFT	CBS-H	CBS-G	CBS-E	CBS-0K	D_0[a]	$\Delta H°f_{(0K)}$[b]	$\Delta H°f_{(298K)}$[c]	γ
NMP+CL	-785,52651	-785,046872	-785,10801	-785,04299	-785,05816	1591,38	-76,70	-83,13	
RC1	-786.22495	-785,049597	-785,09697	-785,05054	-785,05961	1592,29	-77,61	-84,84	
RC2	-786.20098	-785,048959	-785,07562	-785,03140	-785,05975	1592,37	-77,69	-84,44	
RC3	-786.19258	-785,046565	-785,06583	-785,02063	-785,01488	1576,77	-62,09	-84,82	
RC4	-786.18839	-785,046707	-785,06661	-785,02165	-785,01027	1573,87	-59,19	-84,91	
TS1	-786.22013	-785,036605	-785,10076	-785,10076	-785,06557	1596,03	-81,35	-76,69	-534.94
TS2	-786.19486	-785,036199	-785,07739	-785,03414	-785,04222	1581,38	-66,70	-70,43	-732.70
TS3	-786.18378	-785,013008	-785,05664	-785,01395	-785,02207	1566,01	-52,33	-62,16	-1220.71
TS4	-786.17631	-785,015014	-785,059003	-785,01595	-785,02416	1570,04	-55,36	-63,14	-1402.26
PC1	-785,54166	-785,06813	-785,08211	-785,08413	-785,07825	1603,98	-89,30	-96,47	
PC2	-785,54235	-785,06801	-785,10205	-785,08725	-785,05207	1587,55	-72,87	-96,39	
PC3	-785,56214	-785,04135	-785,11012	-785,05625	-785,04094	1580,56	-65,88	-79,66	
PC4	-785,54258	-785,04552	-785,11327	-785,05844	-785,01287	1562,95	-66,27	-82,28	
R1+HCL	-785,49213	-785,06459	-785,12477	-785,06648	-785,07575	1602,42	-87,74	-94,25	
R2+HCL	-785,49397	-785,065363	-785,60168	-135,62446	-785,07773	1603,66	-88,98	-94,73	
R3+HCL	-785,46732	-785,038248	-785,09903	-785,04013	-785,04954	1585,97	-71,29	-77,72	
R4+HCL	-785,47279	-785,044203	-785,10651	-785,04609	-785,05601	1590,03	-75,35	-81,46	

Table 3: Energies (Hartree) of species involved in the Mechanism Obtained at G3B3//B3LYP/6-311G++(2d,pd) Level . CBS-H enthalpy at 298.15 K. CBS-G Gibbs free energy at 298.15 K. CBS-E energy.CBS (0K) energy at 0 K. [a] Atomization energy in kcal mol^{-1} at 0 K. .[b] Heat of formation at 0 K in kcal mol^{-1} . [c] Heat of formation at 298.15 K in kcal mol^{-1}.

	E-DFT	CBS-H	CBS-G	CBS-E	CBS-0K	D_0[a]	$\Delta H°f_{(0K)}$[b]	$\Delta H°f_{(298K)}$[c]	γ (cm^{-1})
NMP+CL	-785,52651	-785,046435	-785,069202	-785,03657	-785,045215	1583,25	-68,57	-82,86	
RC1	-786.22495	-785,07103	-785,04125	-785,04622	-785,05961	1583,88	-69,20	-86,92	
RC2	-786.20098	-785,04622	-785,04622	-785,04622	-785,04622	1587,03	-72,35	-85,49	
RC3	-786.19258	-785,070252	-785,02371	-785,046135	-785,01488	1583,83	-69,15	-85,04	
RC4	-786.18839	-785,070285	-785,02551	-785,051941	-785,01027	1587,47	-72,79	-86,16	
TS1	-786,22013	-785,03661	-785,10076	-785,10076	-785,06557	1596,03	-81,35	-76,69	-534.94
TS2	-786,21486	-785,03404	-785,09858	-785,09499	-785,06326	1594,57	-80,89	-74,53	-732.70
TS3	-786.18378	-785,01254	-785,01532	-785,01209	-785,02207	1577,46	-41,13	-50,41	-1220.71
TS4	-786.17631	-785,01204	-785,02395	-785,01236	-785,02416	1572,63	-42,21	-52,02	-1402.26
PC1	-785,54166	-785,06176	-785,07396	-785,06122	-785,07019	1598,92	-84,24	-92,47	
PC2	-785,54235	-785,06146	-785,07439	-785,06256	-785,07054	1599,14	-84,46	-92,29	
PC3	-785,56214	-785,06042	-785,07439	-785,06959	-785,07014	1598,89	-84,21	-91,63	
PC4	-785,54258	-785,06018	-785,07454	-785,06978	-785,07006	1598,84	-84,16	-91,48	
R1+HCL	-785,49213	-785,052482	-785,081619	-785,059396	-785,058793	1591,77	-77,09	-86,65	
R2+HCL	-785,49397	-785,052162	-785,076229	-135,635732	-785,058571	1591,63	-76,95	-86,45	
R3+HCL	-785,46732	-785,055322	-785,079735	-785,028996	-785,057356	1590,32	-71,64	-85,61	
R4+HCL	-785,47279	-785,027262	-785,075412	-785,026844	-785,033426	1590,85	-73,17	-83,83	

Table 4: ΔH-CBS/ ΔH-G3B3 enthalpy at 298.15 K of reaction NMP+ Cl Obtained at CBS-QB3//B3LYP/6-311G++(2d,pd) / Obtained at G3B3//B3LYP/6-311G++(2d,pd)

	ΔH-CBS	ΔH-G3B3
NMP+CL	0	0
RC1	-1,71	-4,06
RC2	-1,31	-2,63
RC3	-1,69	-2,18
RC4	-1,78	-3,30
TS1	6,44	6,17
TS2	12,7	8,33
TS3	20,97	32,72
TS4	19,99	31,11
PC1	-13,34	-9,61
PC2	-13,26	-9,43
PC3	3,47	-8,77
PC4	0,85	-8,62
R1+HCL	-11,12	-3,79
R2+HCL	-11,6	-3,59
R3+HCL	5,41	-2,75
R4+HCL	1,67	-0,97

Table 5. Rate Constants (cm^3 $molecule^{-1}$ s^{-1}) and Branching Ratio (β) within the Temperature Range 273−380 K for Reaction NMP + Cl at CBS-QB3//B3LYP/6-311G++(2d,pd) .

T	K_I	K_{II}	K*overall*	β1
273	4,87E-10	3,99E-10	8,87E-10	0,55
280	4,93E-10	4,04E-10	8,98E-10	0,55
290	5,02E-10	4,12E-10	9,14E-10	0,55
298	5,09E-10	4,17E-10	9,27E-10	0,55
300	5,11E-10	4,19E-10	9,30E-10	0,55
310	5,20E-10	4,26E-10	9,46E-10	0,55
313	5,22E-10	4,28E-10	9,50E-10	0,55
320	5,28E-10	4,33E-10	9,61E-10	0,55
330	5,37E-10	4,40E-10	9,76E-10	0,55
333	5,39E-10	4,41E-10	9,81E-10	0,55
340	5,45E-10	4,46E-10	9,91E-10	0,55
350	5,53E-10	4,53E-10	1,01E-09	0,55
353	5,55E-10	4,55E-10	1,01E-09	0,55
360	5,61E-10	4,59E-10	1,02E-09	0,55
380	5,77E-10	4,72E-10	1,05E-09	0,55

Table 6. Rate Constants (cm^3 $molecule^{-1}$ s^{-1}) and Branching Ratio (β) within the Temperature Range 273−380 K for Reaction NMP + Cl at G3B3//B3LYP/6-311G++(2d,pd)

T	K_I	K_{II}	$K_{overall}$	β1
273	4,62E-11	4,62E-11	9,24E-11	0,5
280	4,60E-11	4,62E-11	9,22E-11	0,5
290	4,57E-11	4,61E-11	9,18E-11	0,5
298	4,55E-11	4,60E-11	9,16E-11	0,5
300	4,55E-11	4,60E-11	9,15E-11	0,5
310	4,52E-11	4,59E-11	9,11E-11	0,5
313	4,51E-11	4,59E-11	9,10E-11	0,5
320	4,49E-11	4,58E-11	9,07E-11	0,5
330	4,46E-11	4,57E-11	9,03E-11	0,49
333	4,46E-11	4,56E-11	9,02E-11	0,49
340	4,44E-11	4,55E-11	8,99E-11	0,49
350	4,41E-11	4,54E-11	8,94E-11	0,49
353	4,40E-11	4,53E-11	8,93E-11	0,49
360	4,38E-11	4,52E-11	8,90E-11	0,49
380	4,32E-11	4,48E-11	8,81E-11	0,49

Figures

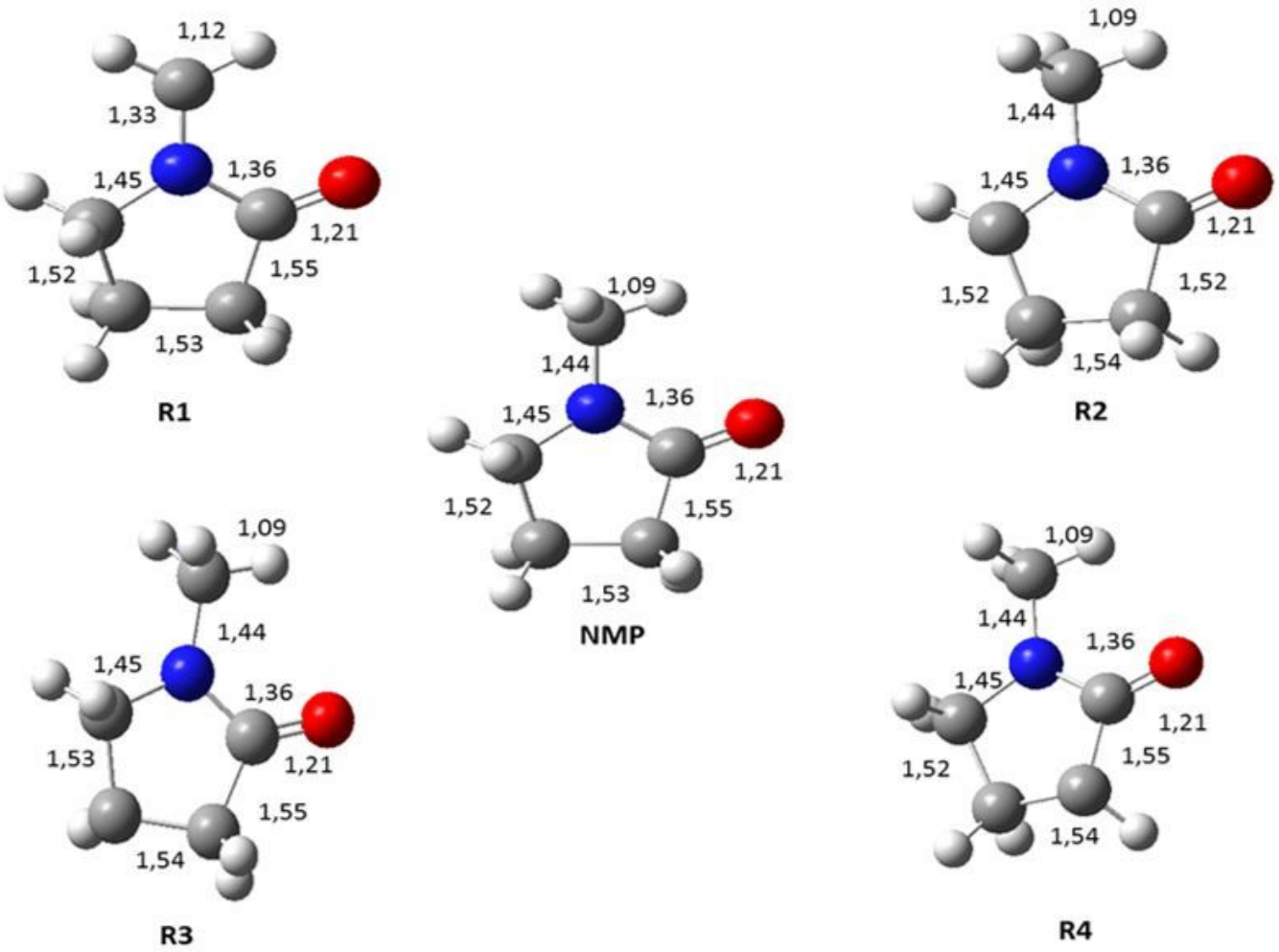

Figure 1

Structures of key species (1-methyl -2-pyrrolidinone –NMP-) and P1–P4 (radicals obtained via channels Ia–Id)) considered for kinetics simulations determined by B3LYP/6-311++G(2d,pd); bond lengths in angstroms.

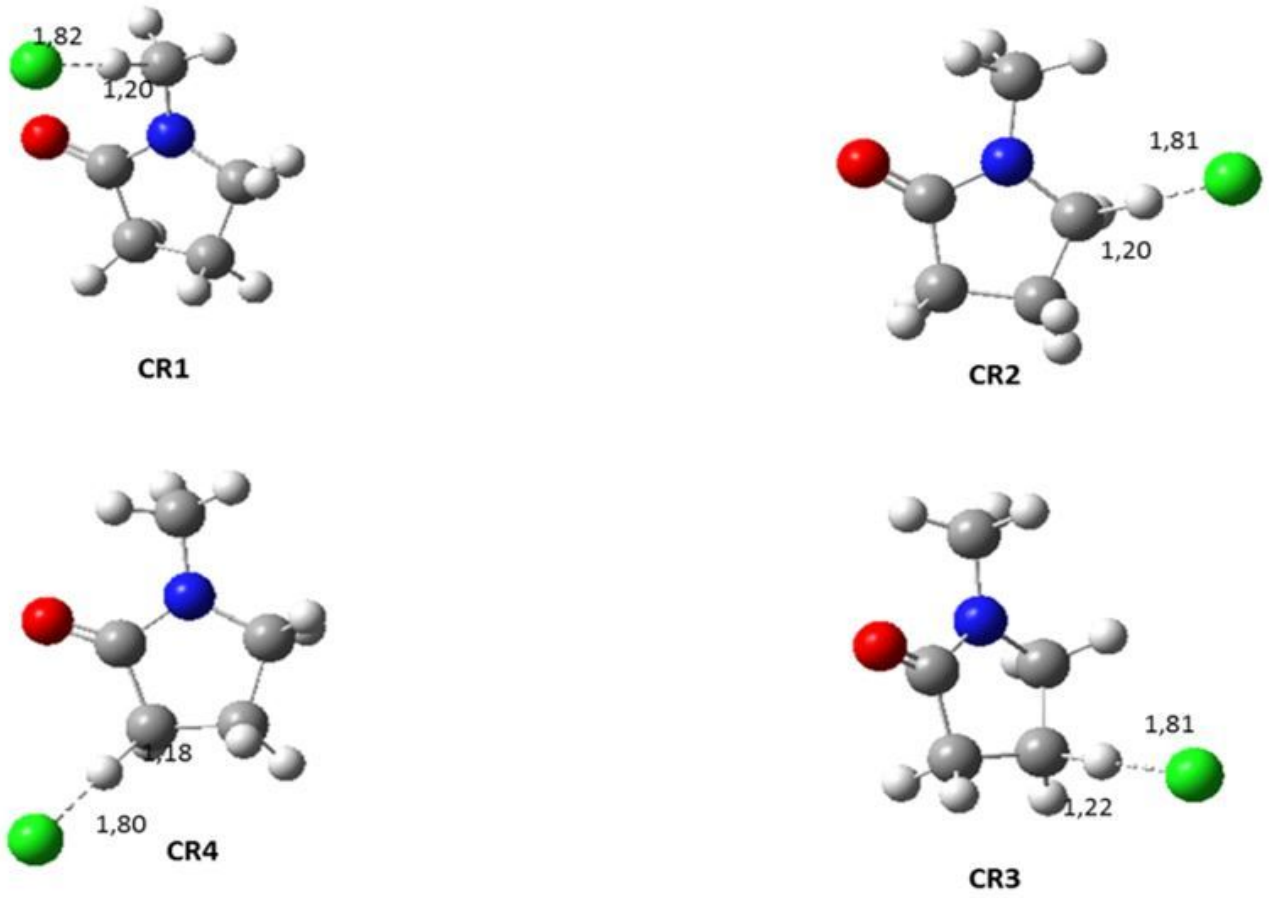

Figure 2

Structures of key species CR1−CR4 (radicals obtained via channels Ia−Id) considered for kinetics simulations determined by B3LYP/6-311++G(2d,pd); bond lengths in angstroms.

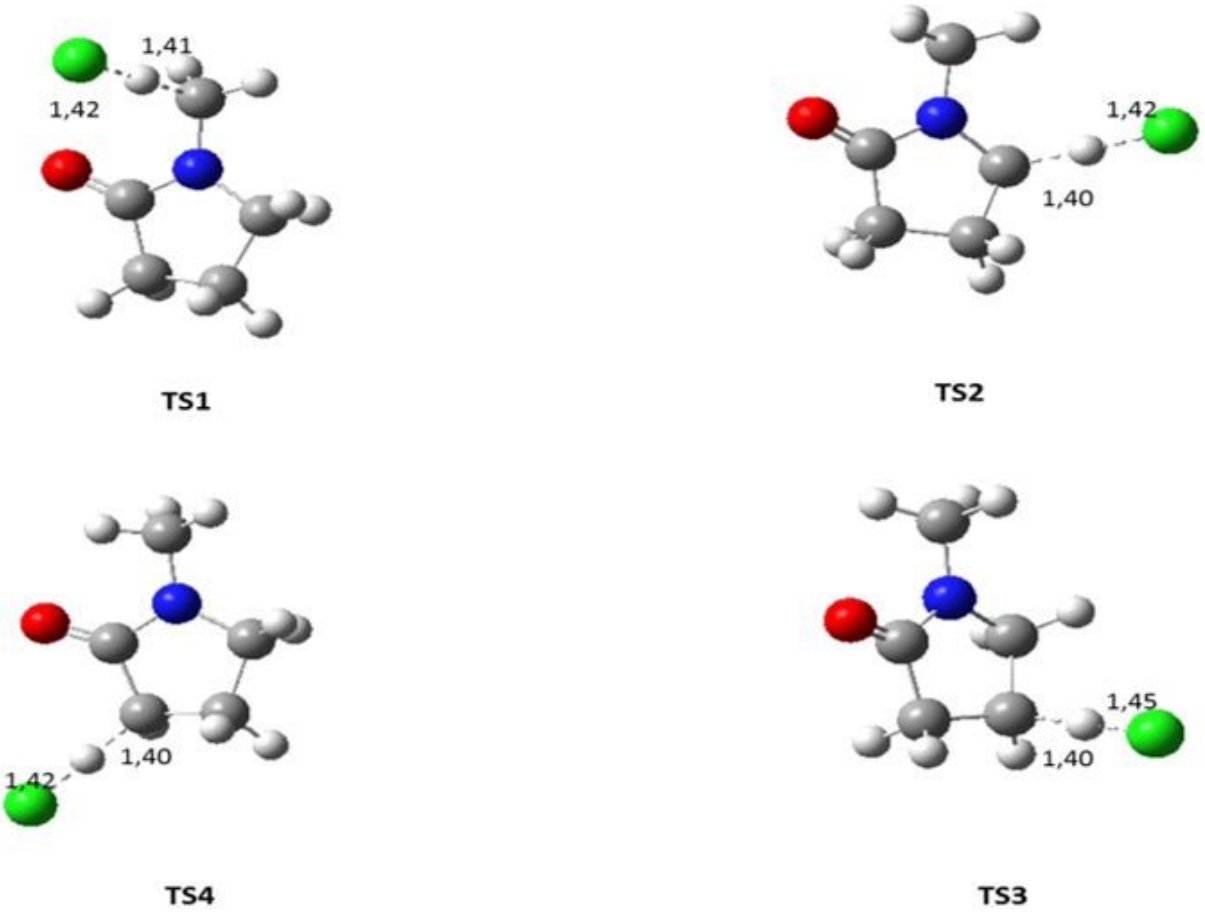

Figure 3

Structures of key species TS1–TS4 (Transitions stat obtained via channels Ia–Id) considered for kinetics simulations determined by B3LYP/6-311++G(2d,pd); bond lengths in angstroms

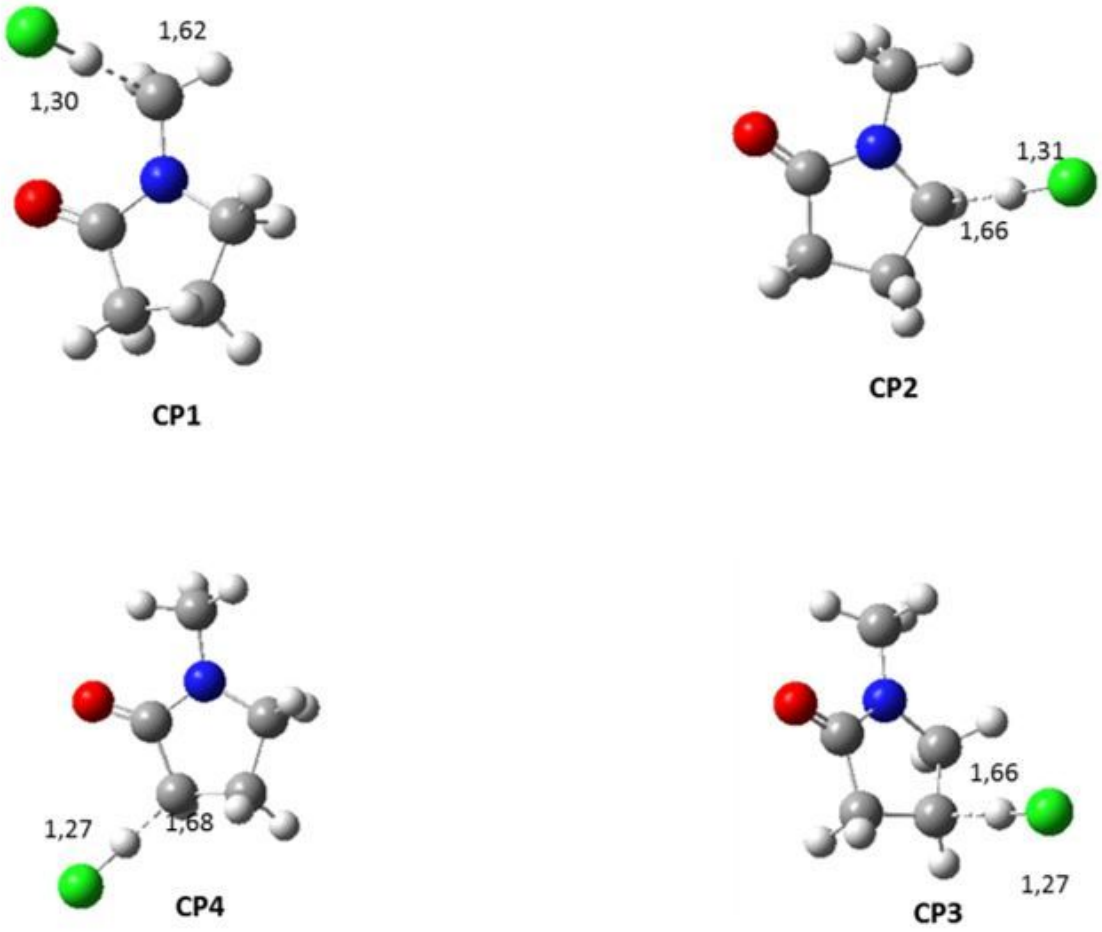

Figure 4

Structures of key species CP1–CP4 obtained via channels Ia–Id considered for kinetics simulations determined by B3LYP/6-311++G(2d,pd); bond lengths in angstroms

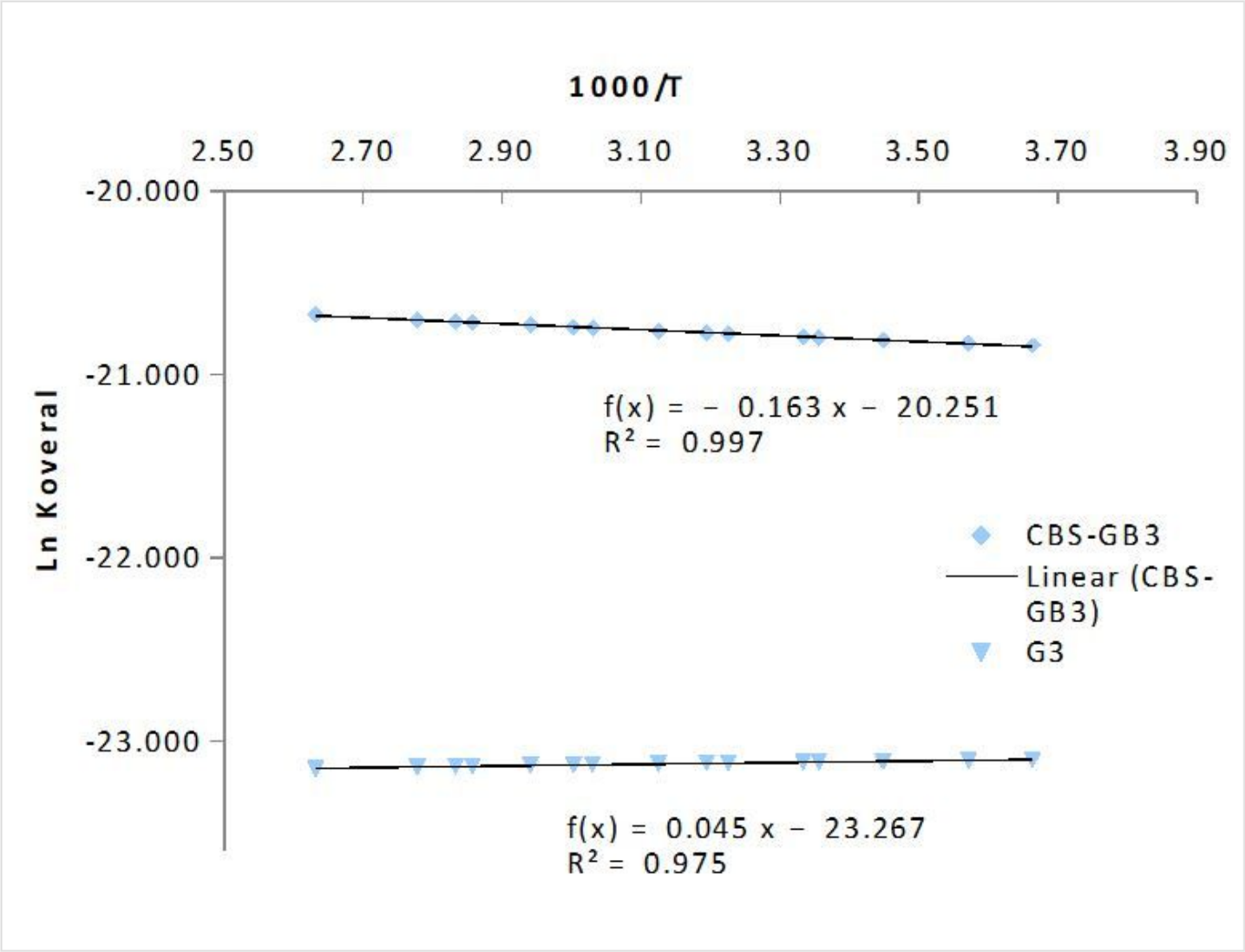

Figure 5

Arrhenius plot ln (koverall) versus 1000/T for NMP + Cl reaction at CBS-QB3 and G3B3

Supplementary Files

This is a list of supplementary files associated with this preprint. Click to download.

- SupportinginformationsNMP.docx